Supporting Information for ***Journal of Materials Chemistry A***

Graphene Coupled Ti_3C_2 MXenes-Derived TiO_2 Mesostructure: Promising Sodium-ion Capacitor Anode with Fast Ion Storage and Long-Term Cycling

Rutao Wang,[a] Shijie Wang,[a] Yabin Zhang,[a] Dongdong Jin,[a] Xinyong Tao,[b] Li Zhang*[a]

[a]Department of Mechanical and Automation Engineering, The Chinese University of Hong Kong, Shatin NT, Hong Kong SAR 999077, P. R. China.

[b]College of Materials Science and Engineering, Zhejiang University of Technology, Hangzhou 310014, P. R. China.

*Email: lizhang@mae.cuhk.edu.hk

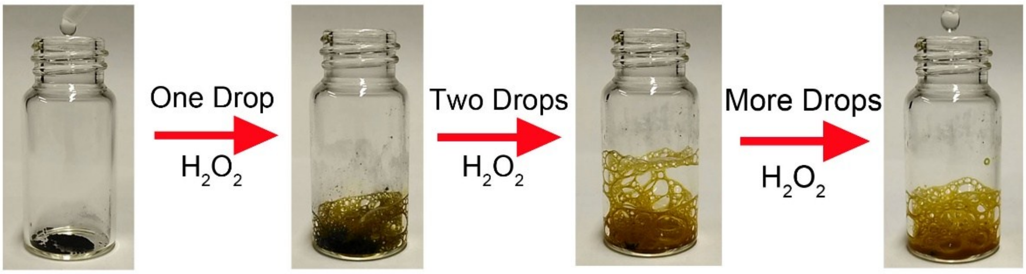

Fig. S1 Optical images showing the violently oxidized process of MXenes-Ti_3C_2 with 30 wt% H_2O_2.

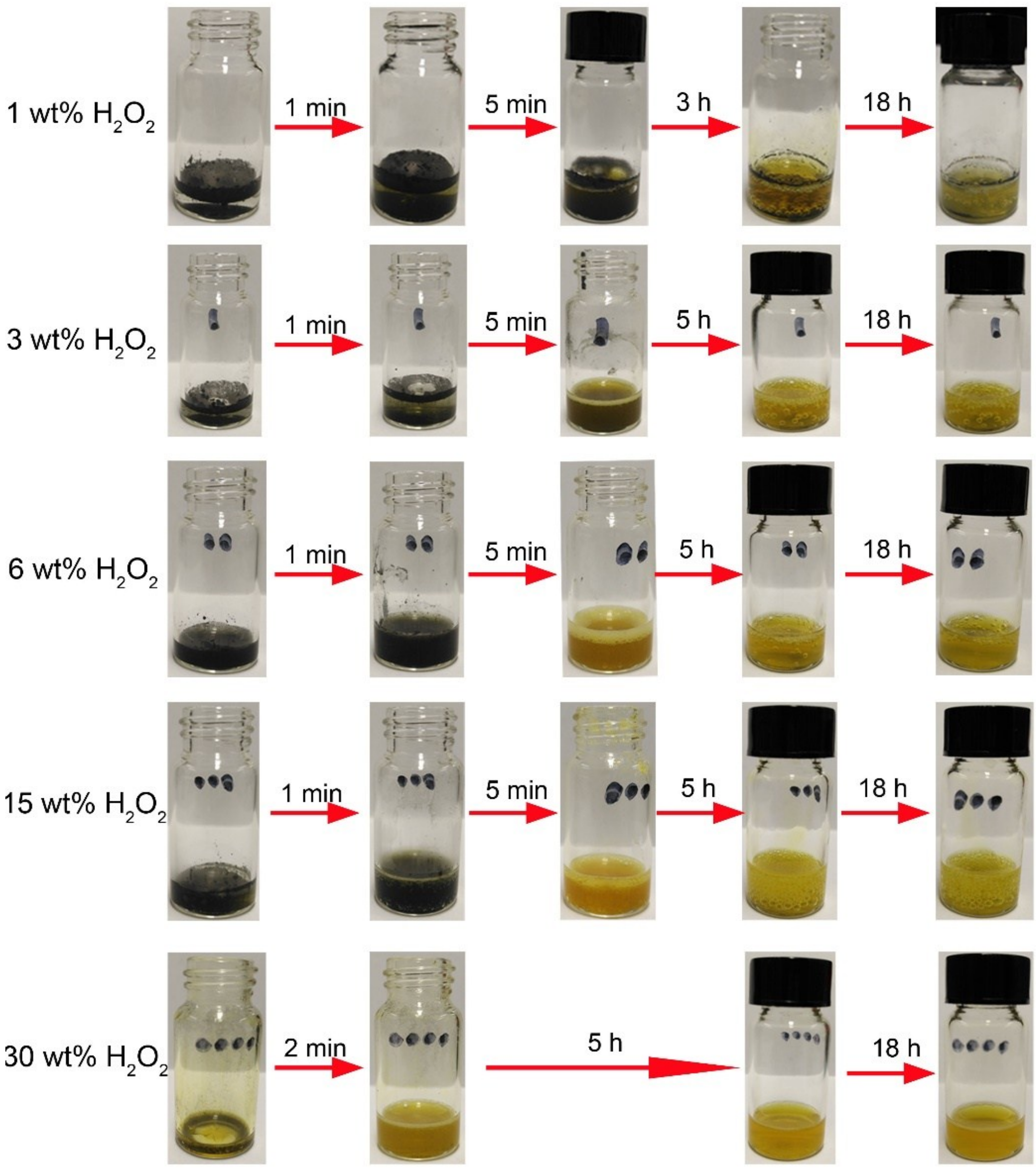

Fig. S2 Optical images showing the reaction process of MXenes-Ti_3C_2 with H_2O_2 with the different concentrations.

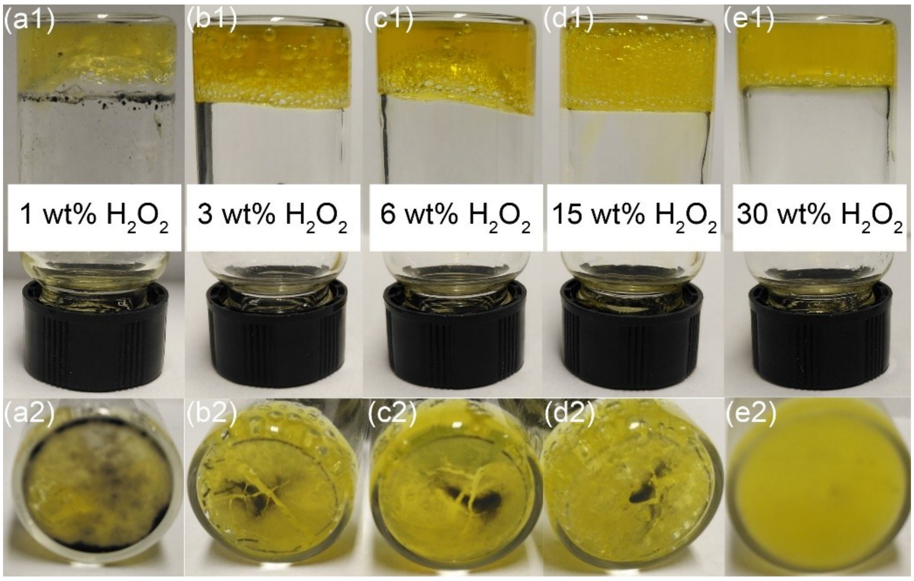

Fig. S3 Optical images showing Ti-peroxo complex gels obtained by the oxidation of H_2O_2 with different concentrations: (a1) and (a2)-1 wt% H_2O_2, (b1) and (b2)-3 wt% H_2O_2, (c1) and (c2)-6 wt% H_2O_2, (d1) and (d2)-15 wt% H_2O_2, (e1) and (e2)-30 wt% H_2O_2. All the gels in the glass bottles can be inverted. Some unreacted raw materials are observed at the bottom of the gels, as the dilute H_2O_2 was used.

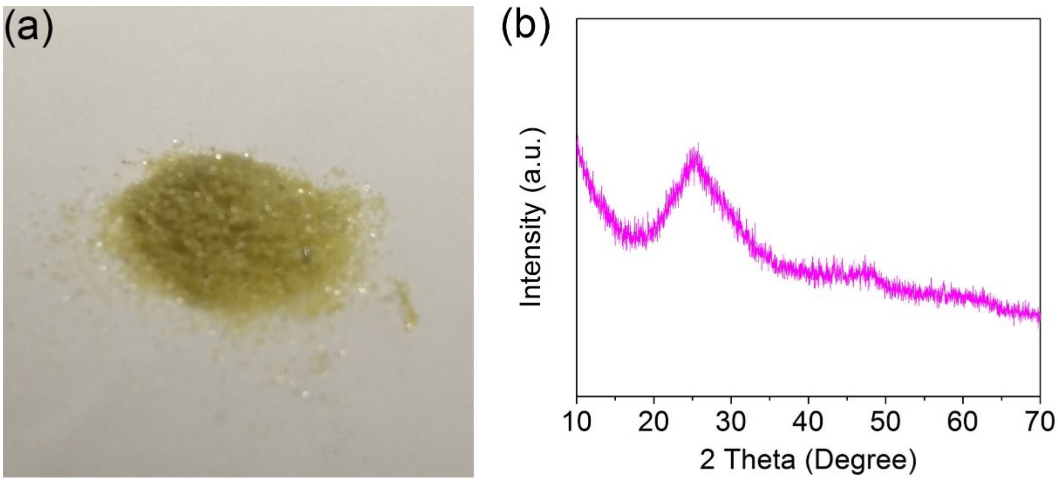

Fig. S4 (a) Optical image and (b) XRD pattern of freeze-dried Ti-peroxo complex gel (from 30 wt% H_2O_2).

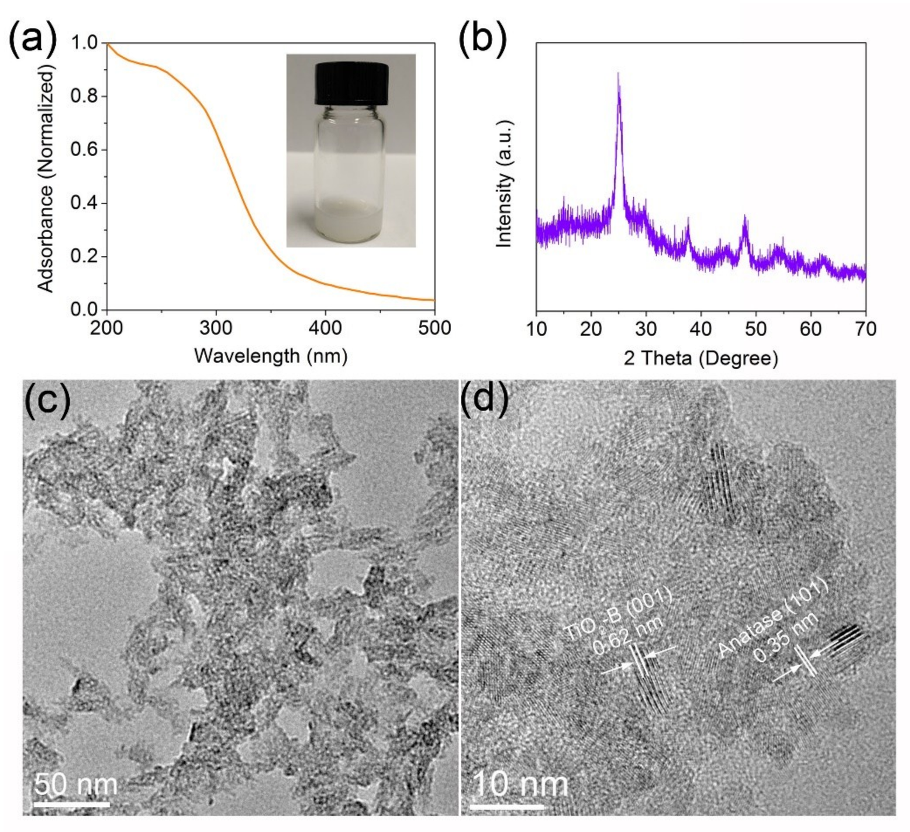

Fig. S5 (a) UV-vis spectrum, (b) XRD pattern, (c) and (d) TEM images of Ti-peroxo complex after aged for two months.

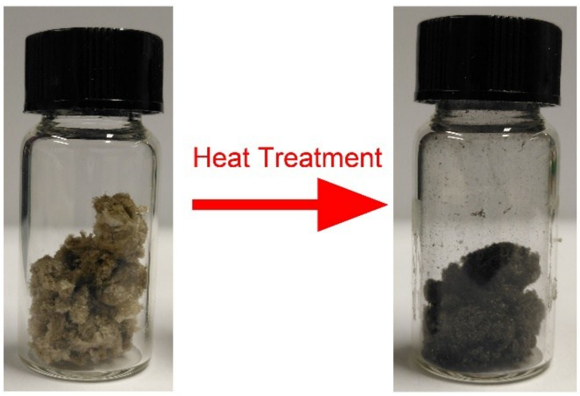

Fig. S6 Optical images for (left) Ti-peroxo complex-GO and (right) M-TiO_2-RGO samples.

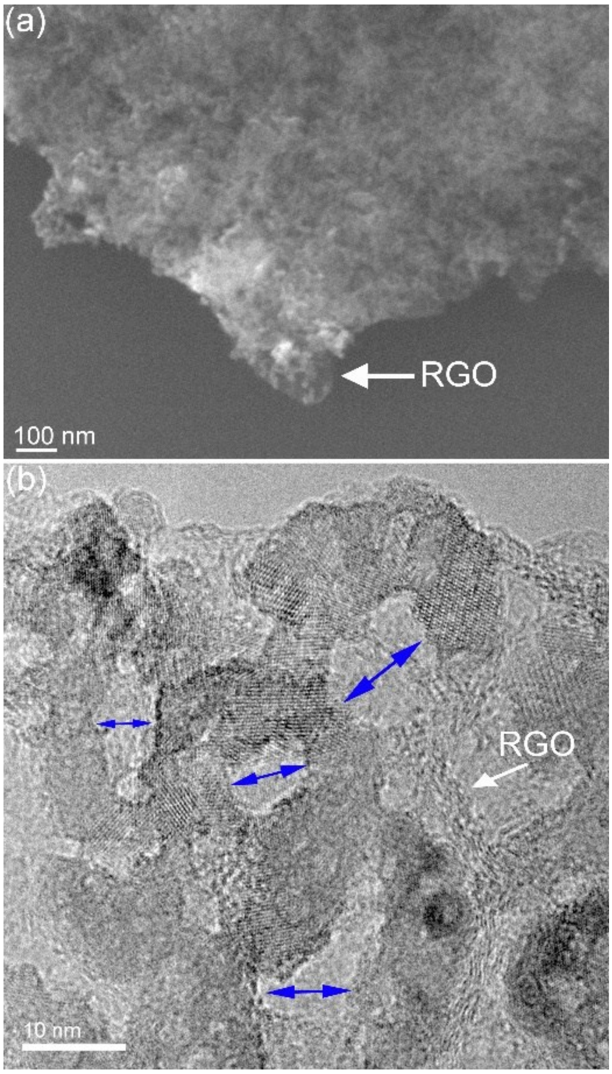

Fig. S7 (a) SEM and (b) HRTEM image of M-TiO_2-RGO. Blue arrows show mesoporous structure in M-TiO_2-RGO.

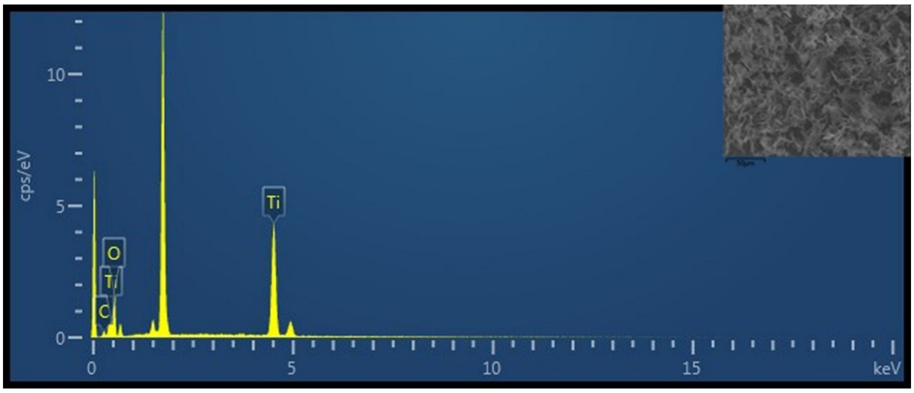

Fig. S8 EDS spectrum of M-TiO_2.

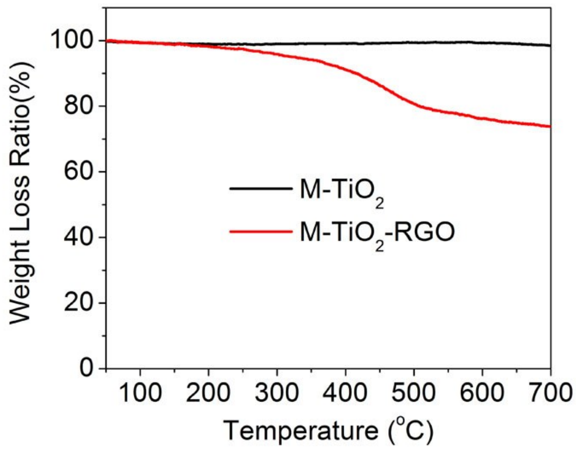

Fig. S9 TGA curves of M-TiO_2 and M-TiO_2-RGO samples in air with an elevated temperature rate of 10^o min^{-1}. The weight loss of M-TiO_2 might be related to the decomposition and oxidation of the residual carbon in air atmosphere. Assuming M-TiO_2 with and without RGO experiences the same weight loss, the content of M-TiO_2 in M-TiO_2-RGO can be calculated as 73.7/98.4=74.9 wt%. The weight retention value here is obtained at 700 ^oC. As we know, RGO can be completely decomposed at 700 ^oC in air. Then the percentage of RGO in M-TiO_2-RGO is (100-74.9) wt%=25.1 wt%.

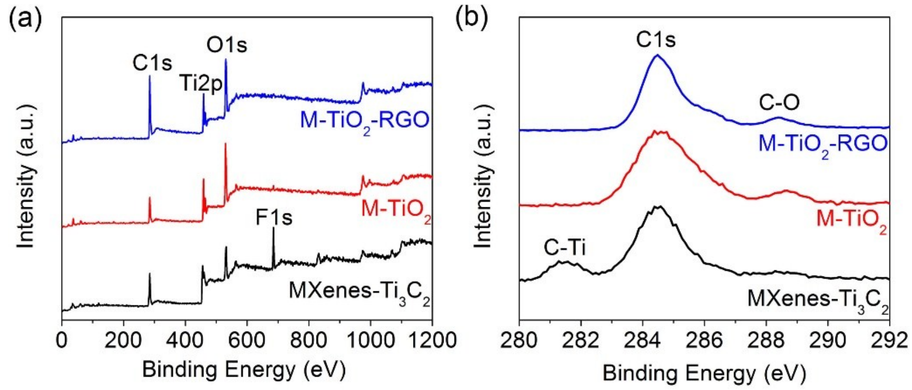

Fig. S10 (a) Full and (b) C1s XPS spectrum of MXenes-Ti_3C_2, M-TiO_2, and M-TiO_2-RGO samples.

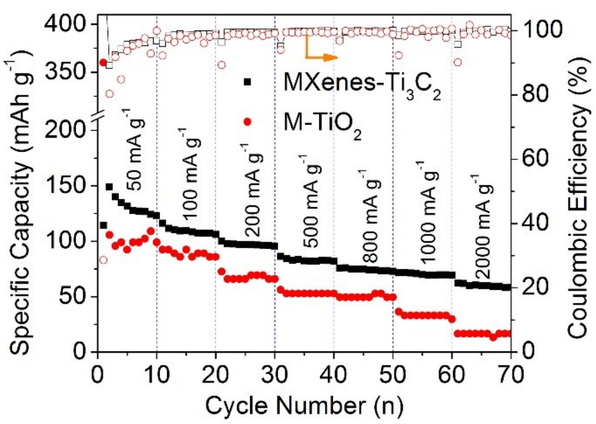

Fig. S11 Rate capability of Ti_3C_2 MXenes and M-TiO_2 at various current densities ranging from 50 to 2000 mA g^{-1}.

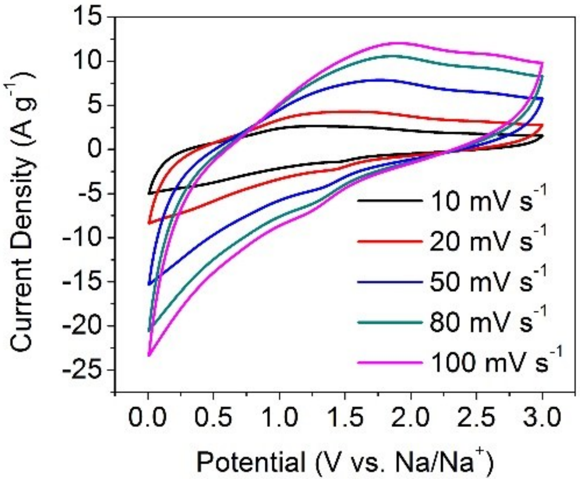

Fig. S12 CV curves from 10 to 100 mV s^{-1} of M-TiO_2-RGO electrode.

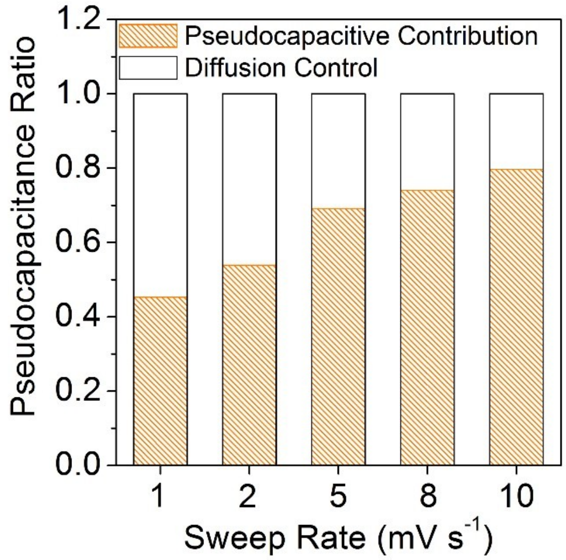

Fig. S13 Contribution ratio of the capacitive and diffusion-controlled charge versus scan rate of M-TiO_2-RGO electrode.

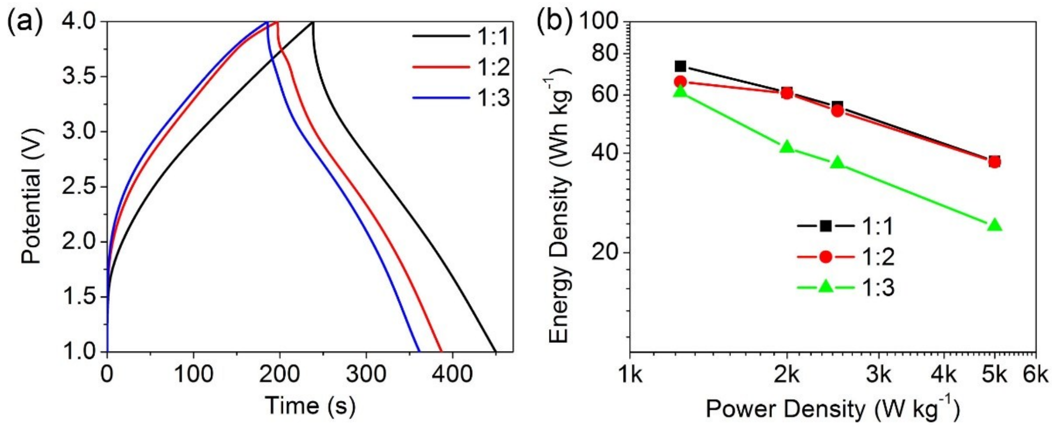

Fig. S14 (a) Galvanostatic charge-discharge curves (current density of 0.5 A g^{-1}) of M-TiO_2-RGO//PDPC SIC measured at different anode/cathode mass ratios. (b) Ragone plot (power density *vs.* energy density) of this M-TiO_2-RGO//PDPC SIC with different anode/cathode mass ratios.